



Published in final edited form as:

*Int J Obes (Lond)*. 2021 July ; 45(7): 1542–1552. doi:10.1038/s41366-021-00818-1.

## Investigation of an ALDH1A1-specific inhibitor for suppression of weight gain in a diet induced mouse model of obesity

Michael Haenisch<sup>1</sup>, Tai Ngyuen<sup>2</sup>, Conrad A. Fihn<sup>2</sup>, Alex S. Goldstein<sup>2</sup>, John K. Amory<sup>3</sup>, Piper Treuting<sup>1</sup>, Thea Brabb<sup>1</sup>, Jisun Paik<sup>1</sup>

<sup>1</sup>Department of Comparative Medicine, University of Washington, Seattle, WA, USA

<sup>2</sup>Focused Scientific, Newcastle, WA, USA

<sup>3</sup>Department of Medicine, University of Washington, Seattle, WA, USA

### Abstract

**Background:** Retinoic acid (RA) controls diverse physiological functions including weight regulation and energy metabolism. It has been reported that mice lacking ALDH1A1, one of the aldehyde dehydrogenases (ALDH) that synthesize RA, are healthy and resistant to weight gain, raising the possibility that inhibiting this enzyme might treat obesity. We previously demonstrated that treatment with a pan-ALDH1A enzyme inhibitor, WIN18446, suppressed weight gain in mice fed a high fat diet (HFD), but caused increased hepatic lipidosis and reversible male infertility.

**Methods:** A series of piperazine compounds that inhibited ALDH1A1 were identified and their inhibitory activity was characterized *in vitro* using purified recombinant enzymes and cell-based assay systems. One potent compound, FSI-TN42 (N42) was examined for its oral bioavailability and pharmacodynamic effects. In addition, its effect on weight gain was investigated by daily oral administration to C57BL/6 male mice receiving a HFD, and compared with mice receiving WIN18446 or vehicle alone (n=6/group, 200 mg compound/kg body weight) for 5 weeks. Body weights were measured weekly, and a glucose tolerance test was performed after 4 weeks of treatment. Tissues were collected to determine changes in adipose weight, hepatic lipidosis, retinoid metabolism, and expression of genes associated with RA and lipid metabolism.

**Results:** N42 irreversibly binds and inhibits ALDH1A1 *in vitro* with a low nM IC<sub>50</sub> and 800-fold specificity for ALDH1A1 compared to ALDH1A2. Daily oral administration of N42 significantly suppressed weight gain (P<0.05) and reduced visceral adiposity (p<0.05) in mice fed a HFD without the hepatic lipidosis observed with WIN18446 treatment.

**Conclusions:** We developed a potent and specific inhibitor of ALDH1A1 that suppressed weight gain in mice fed a HFD. These findings demonstrate that inhibition of ALDH1A1 is a feasible target for drug development to treat and/or prevent obesity.

---

Users may view, print, copy, and download text and data-mine the content in such documents, for the purposes of academic research, subject always to the full Conditions of use: [http://www.nature.com/authors/editorial\\_policies/license.html#terms](http://www.nature.com/authors/editorial_policies/license.html#terms)

Corresponding author: Jisun Paik, 1705 NE Pacific St. HSB, I-604F, Seattle, WA 98195, 206-221-2682, [jpaik@uw.edu](mailto:jpaik@uw.edu).

#### Competing Interests

Authors (Haenisch, Goldstein, Amory, Treuting, and Paik) have filed a patent application (WO2020123855) for FSI-TN42. Ngyuen, Fihn and Brabb declare no potential competing interests.

## Introduction

Obesity has dramatic impacts on public health in the United States and worldwide, affecting morbidity and mortalities associated with the disease such as diabetes, hypertension, dyslipidemia and heart disease(1, 2). A number of different therapies are being employed to induce and maintain weight loss in a sustained manner, such as diet, exercise, surgery, and pharmacological therapy(3, 4). However, only a handful of drugs are approved to treat obesity(5) and thus, additional safe and effective pharmacological treatment could expand treatment options for patients and physicians.

ALDH1A1, along with ALDH1A2 and ALDH1A3, contributes to the synthesis of RA from vitamin A, retinol(6). RA, a ligand for retinoic acid receptors and retinoid X receptors, regulates expression of the genes that are associated with metabolism(7), immunity(8, 9), organogenesis(10) and reproduction(11, 12). Our group has focused on the feasibility of lowering RA levels via inhibition of ALDH1A1 to treat obesity as it has been shown that *Aldh1a1*<sup>-/-</sup> mice are resistant to diet-induced obesity(13–15). We previously reported that an inhibitor of ALDH1A enzymes, WIN18446, reduces weight gain, visceral adiposity and adipocyte size while increasing energy expenditure in mice fed a high-fat diet (HFD)<sup>3</sup>, demonstrating the feasibility of using inhibitors of ALDH1A enzymes to treat obesity. However, we observed that WIN18446 treatment caused hepatic lipidosis as well as inhibition of spermatogenesis leading to reversible male infertility(16, 17). In contrast, *Aldh1a1*<sup>-/-</sup> mice showed decreased hepatic lipidosis when fed a high fat diet (15) and develop and reproduce normally(7). It has been shown that RA required for spermatogenesis are produced by multiple RA synthesis enzymes, *Aldh1a1*, *Aldh1a2* and *Aldh1a3*<sup>11</sup>. Based on these reports, we hypothesized that a specific inhibitor of ALDH1A1 would suppress weight gain without causing hepatic lipidosis or male infertility, potentially providing a safer drug to treat obesity. To test this hypothesis, we developed an ALDH1A1 specific inhibitor, and here, we report its biochemical and pharmacological characterization and efficacy in suppression of weight gain in mice fed a HFD.

## Materials and Methods

### Synthesis of FSI-TN42 (N42 for short, Figure S1)

Chemical reagents were purchased from Sigma-Aldrich, VWR or Chemimpex. Column chromatography was performed using silica gel 60 (230-400 mesh). Analytical TLC was performed using silica gel 60 F<sub>254</sub> precoated on aluminum sheets (0.20mm thickness). <sup>1</sup>H-NMR was recorded using a Bruker 300MHz spectrometer. Chemical shift values are given in ppm. ESMS was performed using a Bruker Esquire mass spectrometer. The final compound was judged to >95% purity based on HPLC-photodiode array detector and gave satisfactory high resolution mass spectrometry (HRMS) using a LTQ-Orbitrap X mass spectrometer.

### RA synthesis enzyme assays

*In vitro* enzyme assays were carried out using purified human ALDH1A1 and ALDH1A2 as previously described with some modification(17, 18). Reactions contained either 5 nM ALDH1A1 or 2 nM ALDH1A2, 300 nM all-*trans* retinal (Toronto Research Chemicals,

North York, Canada), varying concentrations of inhibitors, and 2 mM NAD in 100  $\mu$ L. Retinal was prepared in ethanol (< 0.5% by vol in final reaction) and inhibitors were prepared in DMSO (1% in final reaction). Samples were pre-incubated for 5 min at 37°C, and reactions were initiated by addition of NAD. After additional incubation at 37°C for 5 min (ALDH1A1) or 2 min (ALDH1A2), reactions were quenched by transferring 80  $\mu$ L into an equal volume of acetonitrile containing 100 nM all-*trans* RA5 (Toronto Research Chemicals). All-*trans* RA was quantified using LC-MS as previously described(18). In some experiments, S10 fractions(16) of tissues were used as enzyme sources instead of purified enzymes. For these experiments, 1  $\mu$ M retinal and 15  $\mu$ g (liver, testis and adipose) or 30  $\mu$ g (brain, muscle, lung, lymph node, brown adipose tissue) proteins were used in 300  $\mu$ L total reaction with 15 min incubation. Reactions were quenched by transferring 100  $\mu$ L reaction to 200  $\mu$ L methanol:acetonitrile (1:1, v:v) containing 100 nM all-*trans* RA5. Supernatants (3500xg, 10 min) were collected for LC-MS analysis.

### Tissue culture

ALDH1A enzyme activities were determined using H1299 cells expressing *ALDH1A1* or *ALDH1A2* as described previously(16). Briefly, cells were treated with 1  $\mu$ M retinal and varying concentrations of N42 or WIN18446, and RA production was determined from the culture media 24 h following the treatment.

### Assays to determine interactions between ALDH1A1 and N42

Purified human ALDH1A1 (18  $\mu$ g) was incubated with and without N42 or WIN18446 for 2h at room temperature in a buffer containing 20 mM HEPES, 150 mM KCl, and 1 mM EDTA (pH 8.5) and stored at 4°C. Inhibitors were added to the mixture at 3 times the concentration of ALDH1A1 (mole:mole). Samples (5  $\mu$ L) were analyzed with UPLC (Acquity, Waters) using a Protein BEH C4 column (2.1  $\mu$ m X 150 mm, Waters) and gradient method with running solvents, 0.1% formic acid in water (A) and 0.1% formic acid in acetonitrile (B). Following gradient parameters were used with flow rate at 0.3 ml/min: 0-6 min 97% to 5% A; 6-10 min 5% to 97% A. Intact proteins were detected using SynaptG2-Si TOFMS (Waters) with following conditions: ES+; capillary, 3.5 kV; source temperature, 120 °C; desolvation temperature, 350°C; cone gas flow, 10 L/h; desolvation gas flow, 800 L/h; nebulizer gas flow, 6.5Bar. Leucine enkephalin was used as a reference and TOFMS was set to scan between 2–9.9 min and m/z of 400–3000. The multiple charged series were deconvoluted using MaxEnt software.

### Pharmacokinetics/pharmacodynamics of N42

Male C57BL/6J mice (n=5, 8-10 wo) purchased from the Jackson Laboratory were given N42 by oral installation (dissolved in DMSO and mixed with Nutella). Tail blood was collected at 0.5, 1, 3 and 5 h and plasma was separated and frozen immediately on dry ice. Mice were euthanized by CO<sub>2</sub> asphyxiation 5 h after treatment and tissues collected and frozen.

Circulating N42 levels were determined using an Agilent 1290 UHPLC (Santa Clara, CA) with a Phenomenex C18 column (100 mm x 2.1 mm, 1.7  $\mu$ m particle size) and a SecurityGuard Ultra UHPLC C18 cartridge (Phenomenex, Torrance, CA) held at 40°C.

Running solvents, 0.1% formic acid in water (A) and 0.1% formic acid in acetonitrile (B), were used with flow rate of 0.5 ml/min and with a gradient as follows: 0-1.75 min, 80% A; 1.75-2 min, 80% to 5% A; 2-3.5 min, 5% A; 3.5-5 min, 5% to 80% A. *N*-(3-fluorophenyl)-3-[4-(methylsulfonyl)phenyl]-1-phenyl-1*H*-pyrazole-4-carboxamide was added as an internal standard to each sample. Detection was performed with an AB Sciex5500 qTrap Q-LIT in positive electrospray mode. Ion source parameters were set as follows: declustering potential, 180; curtain gas, 35; medium CAD gas; source temperature, 300°C; GS1, 50; GS2, 60; ion source potential, 5500; exit potential, 10; collision energy, 47; collision exit potential, 13. N42 was detected by the mass transition from 492 to 383 and internal standard by the transition from 436 to 325.

### Animals and diets

C57BL/6J male mice (n=18, 6 week-old, the Jackson laboratory) were acclimated for 1 week in specific pathogen free facility at the University of Washington. Six mice per group was used to detect ~40% differences in weight changes by 3 weeks based on our previous study(16). A list of infectious agents excluded in our facilities were previously reported(19). Mice were housed in individually ventilated cages with corncob bedding with nestlets and provided with an autoclaved standard chow diet (5053, Purina) and chlorinated reverse osmosis automatic water. At 7 weeks of age, mice were switched to a high fat diet (HFD) containing ~60% calories from fat (5WBN, TestDiet, St. Louis, MO, USA) and treated daily with N42 (200 mg/kg), WIN18446 (200 mg/kg) or vehicle (30% peanut oil: 70% Nutella) by oral instillation for 5 weeks. No randomization was performed for the treatment assignment, and experimenters were not blinded to the treatment groups. Weights were determined weekly after the HFD initiation. Fasting glucose and glucose tolerance tests were performed after 4 weeks of treatment as previously described(19). Only male mice were utilized as they are more susceptible to diet-induced obesity than females. All experimental procedures involving animals were approved by the Institutional Animal Care and Use Committee of the University of Washington.

All mice were euthanized by CO<sub>2</sub> asphyxiation after 5-week treatment. Blood, liver, lung, brain, testes, adipose depots (epididymal, retroperitoneal, mesenteric, inguinal, and intrascapular brown adipose tissue) were collected under yellow lights to prevent degradation of retinoids and stored at -80°C for analyses of lipids, retinoids, and/or ALDH1A activities. Individual adipose depots were weighed to determine adiposity, and small pieces of liver were fixed in 10% neutral-buffered formalin for histological analysis. Tissues were processed, sectioned and stained with hematoxylin and eosin (H&E) and Periodic acid – Schiff (PAS) by the Histology and Imaging Core at the University of Washington. Liver lipidosis was scored as previously reported(19) by a veterinary pathologist who was blinded to the treatment groups.

### Triglycerides and retinoid analysis

Serum and liver triglycerides were determined using a colorimetric assay(19), and retinoids in liver, lung and serum were determined as previously reported(17).

## RNA extraction and qRT-PCR

Total RNA preparation, cDNA synthesis and qPCR were carried out as previously described(16).

## Statistical analysis

Statistical analyses were performed with Prism (Graph Pad, La Jolla, CA). All data sets were first tested for normality using Shapiro-Wilk normality test. If data failed the normality test, transformation was attempted. One-way ANOVA or Two-way ANOVA was performed to determine statistical significance ( $p < 0.05$ ). For PD experiments using two different doses or multiple dosing of WIN18446 and N42 (Fig. 2B–F; Fig. S2), two-way ANOVA was used followed by Tukey or Sidak multiple comparison test (Supplemental Table 1). For enzyme activity recovery study (S3) and N42 efficacy study (Fig. 3–5; Fig. S4–5), parametric or non-parametric one-way ANOVA was used depending on normality test followed by Tukey post hoc test adjusting for multiple comparisons. Summary of multiple comparison methods and results for two-way ANOVA are shown in supplemental Table 1.

## Results

### N42 is a specific inhibitor that covalently binds to ALDH1A1.

In our development of novel inhibitors of ALDH1A1, we studied the structure-activity relationship of a series of compounds based on a piperazine scaffold. From these studies, we identified several compounds that inhibited ALDH1A1 but not ALDH1A2. Of these, N42 (Fig. 1A) showed the most promising characteristics as an ALDH1A1-specific inhibitor. We first compared its efficacy and specificity against a known ALDH1A1/1A2 dual inhibitor, WIN18446 (Fig. 1B) using purified recombinant ALDH1A1 and ALDH1A2 (Fig. 1C). In our assay, N42 was 10-fold more potent against recombinant ALDH1A1 than WIN18446 ( $IC_{50}$ , 0.023  $\mu$ M vs 0.25  $\mu$ M). In addition, N42 was 800-fold more potent against ALDH1A1 than ALDH1A2 ( $IC_{50}$ , 0.023  $\mu$ M vs 18  $\mu$ M), while WIN18446 inhibited both ALDH1A1 and 1A2 similarly. Previously, we determined that WIN18446 was a time-dependent inhibitor of ALDH1A1/1A2 and its inhibitory effect was more pronounced with increased incubation time with the enzymes(18). Thus, we developed a cell-based assay to determine long-term cumulative inhibitory effects of inhibitors(16). While WIN18446 and N42 were similarly potent against ALDH1A1 in cells (0.06  $\mu$ M  $EC_{50}$ , Fig. 1D), only WIN18446 inhibited ALDH1A2. In addition, cells treated with N42 did not recover RA synthesis activity by ALDH1A1 after washout of the compound similarly to the cells treated with WIN18446 (Fig. 1E). To confirm that N42 binds ALDH1A1 irreversibly, we analyzed mixtures of ALDH1A1 and N42 compared to enzyme alone using UPLC-TOFMS. ALDH1A1 incubated with N42 showed a mass shift equal to addition of the inhibitor with loss of ~70 amu, approximately two chlorides (Fig. 1F vs. G). As expected, we observed a similar mass shift with WIN18446 (Fig. 1F vs. H).

### N42 is orally bioavailable and inhibits ALDH1A1 *in vivo*.

Mice dosed orally with 10 mg/kg N42 show peak plasma concentrations at 1h and a terminal half-life of 6-10 h (Fig. 2A). However, plasma concentrations did not exceed nM levels,

suggesting that N42 may have low oral bioavailability or high metabolism in the gut. Because the  $IC_{50}$  of N42 is ~20 nM, we determined the pharmacodynamic effects of this compound by measuring RA synthesis capacity in S10 fractions from two target organs for obesity, liver and epididymal adipose, at two dosing levels (Fig. 2B, C). Tissues collected 5 h after oral treatment of N42 showed decreased RA synthesis activity at both low (10 mg/kg) and high (200 mg/kg) doses, with the higher dose having a more pronounced effect in liver (Fig. 2B), but not in epididymal adipose (Fig. 2C). WIN18446 showed stronger suppression of RA synthesis in liver compared to N42 as it inhibits both ALDH1A1 and ALDH1A2. In epididymal adipose, N42 reduced RA synthesis to a similar degree as WIN18446, but neither showed more than a 30% reduction. These data demonstrate pharmacodynamic effects of N42 despite its low serum response following oral dosing.

We next determined pharmacodynamics of N42 after multiple dosing. Mice were orally given 200 mg/kg N42 or WIN18446 daily for either 1 day or 7 days, and tissues were collected 24 h after the last dose to determine RA synthesis capacity of various tissues. Both single and multiple dosing of N42 resulted in significant suppression of RA synthesis in multiple tissues (Fig. 2D–F, Fig. S2). Both WIN18446 and N42 reduced RA synthesis activity in the liver (Fig. 2D) and epididymal adipose tissue (Fig. 2E) after both single and multiple dosing. RA synthesis activity tended to be reduced in other adipose depots of mice treated with N42 or WIN18446 (Fig. S2A–C). Interestingly, N42 had no effect on testis RA synthesis activity while WIN18446 eliminated almost all activity (Fig. 2F). In addition, WIN18446 strongly inhibited RA synthesis in brain regardless of dosing regimen while N42 treatment showed an accumulating suppressive effect on RA activity after multiple dosing (Fig. S2D). Suppression of RA synthesis was also less pronounced compared to WIN18446 in skeletal muscle (Fig. S2E) and mesenteric lymph node (Fig. S2F).

Since N42 strongly and irreversibly binds to ALDH1A1 (Fig. 1G), it is expected to have long-lasting pharmacodynamic effects as enzyme activity is able to recover only when new unbound proteins are synthesized. Thus, we sought to measure the duration of RA synthesis inhibition by N42 *in vivo* compared to WIN18446 (Fig. 2G–I, Fig. S3). In most tissues, inhibitory effects of N42 were sustained up to 72h, comparable to that of WIN18446 treatment.

### **N42 protects against diet-induced obesity.**

Pharmacodynamic studies suggested that N42 can significantly and specifically inhibit ALDH1A1 *in vivo*, potentially reducing side effects from comparable WIN18446 treatment. We thus tested efficacy of N42 in obesity by feeding C57BL/6J male mice a HFD and treating them with N42, WIN18446 or vehicle control by daily oral instillation. After 5 weeks of treatment, both N42 and WIN18446 reduced weight gain compared to vehicle treated controls although only N42 treatment reached statistical significance (Fig. 3A). Both compounds significantly reduced visceral (Fig. 3B–D) and subcutaneous adipose gain (Fig. 3E), resulting in reduction of visceral adiposity from 7.7 % in controls to 5.0 % and 5.2 % in WIN18446 and N42-treated mice, respectively (Fig. 3G). Brown adipose tissue weights were similar between treatment groups (Fig. 3F). Consistent with our previous reports(16, 17, 20), treatment with WIN18446 significantly reduced testes mass while testes of mice



treated with N42 were unaffected (Fig. 3H). Fasting glucose and AUC in a glucose tolerance test were unaffected by either treatment (Fig. S4).

Previously, we showed that WIN18446 treatment reduced circulating levels of triglycerides while increasing hepatic triglycerides(16, 17). Therefore, we histologically examined liver and measured hepatic and circulating triglycerides after the five-week treatment. Due to the shorter period of HFD feeding, lipidosis in control livers was not as pronounced as we have seen after longer periods of HFD feeding (mostly scores of 1-2 in this study vs. 2-4 previously). However, after only 5 weeks of treatment, we observed increased lipidosis in WIN18446 treatment, while N42 suppressed lipidosis (Fig. 4A, B). Liver weight as a percentage of body weight was also increased by treatment with WIN18446 (Fig. 4C). In agreement with these observations, liver triglycerides tended to be higher in WIN18446 treatment and lower in N42 treatment although these differences did not reach statistical significance (Fig. 4D). In contrast, circulating levels of triglycerides were higher in mice treated with N42 but not those treated with WIN18446 (Fig. 4E). We also determined expression levels of genes associated with lipid metabolism in liver, but did not observe any significant changes in these genes (Fig. S5A–C).

#### **N42 affects retinoid storage and metabolism in a tissue-dependent manner.**

We reported that RA synthesis inhibition by a dual ALDH1A1/1A2 inhibitor, WIN18446, affected tissue retinoid metabolism(16, 17). Since N42 is a specific inhibitor of ALDH1A1, we wanted to determine if and how N42 changed tissue retinoids compared to WIN18446. We determined retinyl ester and retinol levels in liver and lung, the two organs that normally store high concentrations of retinyl esters (Table 1). As previously reported, WIN18446 significantly reduced levels of retinol and retinyl esters in lung. N42 also significantly reduced retinyl ester levels in lungs, albeit not as dramatically as WIN18446, but it did not alter retinol levels. Either WIN18446 or N42 treatment did not influence retinyl ester levels while only WIN18446 decreased retinol levels in the liver. Circulating levels of retinol were not significantly different between the groups.

Next, we determined pharmacodynamics of N42 compared to WIN18446 in various tissues after the 5wk of daily oral treatment (Fig. 5). N42 significantly suppressed RA synthesis activity in liver, lung, brain and to a lesser extent in testis. However, neither compound significantly suppressed RA synthesis activity of epididymal adipose. In agreement with the multiple dosing study, inhibition of RA synthesis was generally stronger in tissues of mice treated with WIN18446 compared to N42. Since N42 strongly altered retinoid levels and RA synthesis activity in liver and lung, we then determined expression levels of genes influenced by RA in these tissues using qPCR (*Lrat* and *Cyp26a1*) as surrogate measures of RA. *Cyp26a1* expression was significantly reduced by treatment with either compound in liver (Fig. 5B) while only *Lrat* was significantly reduced by WIN18446 in lung. To determine whether there is a compensatory increase in gene expression of *Aldh1a1* or *Aldh1a2* enzymes in response to the suppression of their activity, we determined the expression levels of *Aldh1a1* or *1a2* in liver and lungs (Fig. S5D–G). Expression levels of *Aldh1a1* are higher than *Aldh1a2* in both tissues and inhibitor treatment did not influence

expression of either enzyme except for a statistically significant increase in *Aldh1a2* expression following WIN18446 treatment in liver.

## Discussion

We reported previously that mice treated with the dual ALDH1A1/1A2 inhibitor, WIN18446, were resistant to weight gain on both high(16) and low-fat diets(17). Despite its efficacy in weight suppression, WIN18446 causes significant side effects including spermatogenesis blockage, hepatic lipidosis and alcohol intolerance(17), making it an unlikely candidate for further development as an obesity treatment. Because *Aldh1a1*<sup>-/-</sup> mice are resistant to diet-induced obesity(13–15), we hypothesized that WIN18446 exerts its effects on weight gain through inhibition of ALDH1A1. Since *Aldh1a1*<sup>-/-</sup> mice reproduced normally and are healthy, we also hypothesized that ALDH1A1-specific inhibitors may avoid side effects from WIN18446 treatment. Therefore, we developed novel specific inhibitors of ALDH1A1 and tested the efficacy of one such molecule in a diet-induced model of obesity.

Crystallographic studies of WIN18446 show that it blocks the active site of ALDH1A2 through the formation of a covalent bond made from displacement of a chloride by the active site cysteine(21). N42 was synthesized by combining the dichloroacetamide group of WIN18,446 with the bulkier piperazine scaffold to bias the inhibition selectivity toward ALDH1A1 which has a larger substrate binding pocket than ALDH1A2 (22). The mass shift observed with protein mass-spectrometry in our study (Fig. 1G) suggests that N42 may inhibit ALDH1A1 through a similar mechanism seen with WIN 18,446. This interpretation is also supported by the fact that ALDH1A1 activity does not recover after washout of N42 in cells (Fig. 1E). We do not know why N42 does not inhibit ALDH1A2 through the same mechanism. One possibility is that the smaller substrate binding pocket of ALDH1A2 may not accommodate N42 which is bulkier and conformationally more restricted than WIN18446. Despite the low serum levels of N42 following oral dosing (Fig. 2A), N42 showed strong pharmacodynamic effects against ALDH1A1 in various tissues (Fig. 2, S2–3) which was sustained for a long period (24 - 72 h depending on tissues) likely due to its irreversible binding to ALDH1A1. Both WIN18446 and N42 appear to cross blood-brain barrier as they significantly inhibited RA synthesis capacity in brain (Fig. S3). We plan to investigate central nervous system mediated weight regulation by ALDH1A inhibitors in the future. We observed a rapid decline in plasma concentrations of N42 from 1-3h after a single oral dose (Fig 2A), which also suggests that the compound may accumulate inside tissues as N42 gets bound to ALDH1A1 tightly rather than reaching equilibrium between plasma and tissue. Future studies are needed to determine precise mechanisms of pharmacokinetics and pharmacodynamics.

We did not observe any significant clinical signs of adverse effects due to N42 administration based on daily monitoring of body conditions and weekly weight changes. Daily oral administration of N42 for 5 weeks was sufficient to reduce weight gain and visceral adiposity in mice fed HFD. The same dose of WIN18446 also suppressed weight gain in mice although it did not reach statistical significance. We have previously shown that mice fed a diet containing WIN18446 had significantly reduced weight gain after only three



weeks of treatment(16). In that study, WIN18446 was administered to mice in the diet after mice had already become obese from 8 weeks of feeding HFD. The differences in efficacy may be due to more favorable pharmacodynamic effects of WIN18446 achieved from its constant supply through diet. Additionally, it is possible that significant adiposity suppression can be more easily detected when mice are beyond the rapid growth phase. These data suggest that inhibition of ALDH1A1 can suppress weight gain through decrease in fat mass gain as previously reported(16, 19).

One side effect of WIN18446 treatment was increased hepatic lipidosis(16, 19), which differed from the phenotype of *Aldh1a1*<sup>-/-</sup> mice with reduced hepatic lipidosis(15). We thus hypothesized that exacerbation of hepatic lipidosis seen in WIN18446 treated mice might be due to off-target effects rather than its inhibition of ALDH1A1. Indeed, treatment with N42, an ALDH1A1 specific inhibitor, tends to reduce hepatic lipidosis (Fig. 4). Further studies with longer treatment duration will be needed to confirm this finding. Unexpectedly, we observed increased serum TG levels in mice treated with N42. We do not know mechanisms by which this occurs at this time and future studies will explore potential mechanisms including VLDL synthesis and tissue uptake (lipoprotein lipase). Another side effect of WIN18446 treatment was spermatogenesis blockage that is associated with significant reduction in testes weight(16, 19). We again observed significant reductions in testis weight in mice treated with WIN18446 after 5 weeks treatment. In contrast, the same exposure to N42 did not alter testes weight (Fig. 3H). Although ALDH1A1 contributes to ~50% of RA synthesis capacity of testis(23), *Aldh1a1*<sup>-/-</sup> mice are fertile (24), suggesting that ALDH1A1 is dispensable in spermatogenesis. Thus, our data also support the notion that ALDH1A1-specific inhibitors would not inhibit spermatogenesis and thus, male fertility. Future studies will be needed to confirm fertility of mice treated with N42 by histology and mating studies. While we did not expect to see any significant effects on testis weight by ALDH1A1-specific inhibitors as *Aldh1a1a*<sup>-/-</sup> mice reproduce normally, we were surprised to find that N42 did not result in significant suppression of RA synthesis activity in testes after multiple dosing (Fig. 2F). Even after 5 weeks treatment with N42, only three out of six mice showed a 15-50% reduction in RA synthesis in testes (Fig. 5H). This was unexpected because N42 can strongly inhibits testicular ALDH1A1 when it is directly added to testis homogenates *in vitro* (60-70% reduction; data not shown). One plausible explanation is that N42 is not taken up by testis as easily as other tissues. Further studies will be needed to address mechanisms behind this observation.

While tissue RA measurement is a definitive indicator of the consequences of ALDH1A inhibition, tissue levels of RA are difficult to measure due to extremely low levels. RA is also light sensitive and extraction efficiency is influenced by many factors(25, 26). To circumvent this problem, we previously measured ALDH1A activity in fractions containing cytosolic proteins (S10) of tissue homogenates from mice as surrogate measures of functional ALDH1A enzymes(16). Using this method, we determined that an ALDH1A1 specific inhibitor, N42, reduced the majority of RA synthesis in liver (>75%, Fig. 2, 5) but only modestly reduced the activity in adipose tissue (~30%). Our data provide a possible explanation as to why *Aldh1a1*<sup>-/-</sup> mice had a ~50% reduction in liver RA levels but no statistically significant changes in adipose RA levels compared to WT mice(14).

In summary, we demonstrate that it is possible to develop a specific and potent inhibitor of ALDH1A1 despite the high structural similarity between ALDH1A1 and ALDH1A2. We also show evidence that such compounds can be used to suppress weight gain. Further studies will be needed to assess long-term safety, optimal dosing, and potential off-target effects of N42 for treatment of obesity.

## Supplementary Material

Refer to Web version on PubMed Central for supplementary material.

## Acknowledgements

This work was supported by the National Institute of Health (NIH) grant (R56 DK110239-01A1). Protein mass analysis was performed at Mass Spectrometry Center (School of Pharmacy, UW) and liver histology was performed at Histology Imaging Core (Department of Comparative Medicine, UW).

## References

1. Malnick SD, Knobler H. The medical complications of obesity. *QJM*. 2006;99(9):565–79. [PubMed: 16916862]
2. Apovian CM. Obesity: definition, comorbidities, causes, and burden. *Am J Manag Care*. 2016;22(7 Suppl):s176–85. [PubMed: 27356115]
3. Jackson VM, Breen DM, Fortin JP, Liou A, Kuzmiski JB, Loomis AK, et al. Latest approaches for the treatment of obesity. *Expert Opin Drug Discov*. 2015;10(8):825–39. [PubMed: 25967138]
4. Kushner RF. Weight Loss Strategies for Treatment of Obesity: Lifestyle Management and Pharmacotherapy. *Prog Cardiovasc Dis*. 2018;61(2):246–52. [PubMed: 29890171]
5. Velazquez A, Apovian CM. Updates on obesity pharmacotherapy. *Ann N Y Acad Sci*. 2018;1411(1):106–19. [PubMed: 29377198]
6. Blaner WS. Vitamin A signaling and homeostasis in obesity, diabetes, and metabolic disorders. *Pharmacol Ther*. 2019;197:153–78. [PubMed: 30703416]
7. Zhang R, Wang Y, Li R, Chen G. Transcriptional Factors Mediating Retinoic Acid Signals in the Control of Energy Metabolism. *Int J Mol Sci*. 2015;16(6):14210–44. [PubMed: 26110391]
8. Canete A, Cano E, Munoz-Chapuli R, Carmona R. Role of Vitamin A/Retinoic Acid in Regulation of Embryonic and Adult Hematopoiesis. *Nutrients*. 2017;9(2).
9. Pino-Lagos K, Benson MJ, Noelle RJ. Retinoic acid in the immune system. *Ann N Y Acad Sci*. 2008;1143:170–87. [PubMed: 19076350]
10. Ghyselinck NB, Duester G. Retinoic acid signaling pathways. *Development*. 2019;146(13).
11. Yadu N, Kumar PG. Retinoic acid signaling in regulation of meiosis during embryonic development in mice. *Genesis*. 2019;57(7–8):e23327. [PubMed: 31313882]
12. Teletin M, Vernet N, Ghyselinck NB, Mark M. Roles of Retinoic Acid in Germ Cell Differentiation. *Curr Top Dev Biol*. 2017;125:191–225. [PubMed: 28527572]
13. Kiefer FW, Vernochet C, O'Brien P, Spoerl S, Brown JD, Nallamshetty S, et al. Retinaldehyde dehydrogenase 1 regulates a thermogenic program in white adipose tissue. *Nature medicine*. 2012;18(6):918–25.
14. Yang D, Krois CR, Huang P, Wang J, Min J, Yoo HS, et al. Raldh1 promotes adiposity during adolescence independently of retinal signaling. *PLoS One*. 2017;12(11):e0187669. [PubMed: 29095919]
15. Ziouzenkova O, Orasanu G, Sharlach M, Akiyama TE, Berger JP, Viereck J, et al. Retinaldehyde represses adipogenesis and diet-induced obesity. *Nature medicine*. 2007;13(6):695–702.
16. Haenisch M, Treuting PM, Brabb T, Goldstein AS, Berkseth K, Amory JK, et al. Pharmacological inhibition of ALDH1A enzymes suppresses weight gain in a mouse model of diet-induced obesity. *Obes Res Clin Pract*. 2018;12(1):93–101. [PubMed: 28919001]

17. Paik J, Haenisch M, Muller CH, Goldstein AS, Arnold S, Isoherranen N, et al. Inhibition of retinoic acid biosynthesis by the bisdichloroacetyldiamine WIN 18,446 markedly suppresses spermatogenesis and alters retinoid metabolism in mice. *The Journal of biological chemistry*. 2014;289(21):15104–17. [PubMed: 24711451]
18. Arnold SL, Kent T, Hogarth CA, Schlatt S, Prasad B, Haenisch M, et al. Importance of ALDH1A enzymes in determining human testicular retinoic acid concentrations. *Journal of lipid research*. 2015;56(2):342–57. [PubMed: 25502770]
19. Paik J, Fierce Y, Drivdahl R, Treuting PM, Seamons A, Brabb T, et al. Effects of murine norovirus infection on a mouse model of diet-induced obesity and insulin resistance. *Comparative medicine*. 2010;60(3):189–95. [PubMed: 20579433]
20. Amory JK, Muller CH, Shimshoni JA, Isoherranen N, Paik J, Moreb JS, et al. Suppression of spermatogenesis by bisdichloroacetyldiamines is mediated by inhibition of testicular retinoic acid biosynthesis. *Journal of andrology*. 2011;32(1):111–9. [PubMed: 20705791]
21. Chen Y, Zhu JY, Hong KH, Mikles DC, Georg GI, Goldstein AS, et al. Structural Basis of ALDH1A2 Inhibition by Irreversible and Reversible Small Molecule Inhibitors. *ACS Chem Biol*. 2018;13(3):582–90. [PubMed: 29240402]
22. Lamb AL, Newcomer ME. The structure of retinal dehydrogenase type II at 2.7 Å resolution: implications for retinal specificity. *Biochemistry*. 1999;38(19):6003–11. [PubMed: 10320326]
23. Arnold SL, Kent T, Hogarth CA, Griswold MD, Amory JK, Isoherranen N. Pharmacological inhibition of ALDH1A in mice decreases all-trans retinoic acid concentrations in a tissue specific manner. *Biochem Pharmacol*. 2015;95(3):177–92. [PubMed: 25764981]
24. Raverdeau M, Gely-Pernot A, Feret B, Dennefeld C, Benoit G, Davidson I, et al. Retinoic acid induces Sertoli cell paracrine signals for spermatogonia differentiation but cell autonomously drives spermatocyte meiosis. *Proc Natl Acad Sci U S A*. 2012;109(41):16582–7. [PubMed: 23012458]
25. Kane MA, Chen N, Sparks S, Napoli JL. Quantification of endogenous retinoic acid in limited biological samples by LC/MS/MS. *Biochem J*. 2005;388(Pt 1):363–9. [PubMed: 15628969]
26. Kane MA, Folias AE, Wang C, Napoli JL. Quantitative profiling of endogenous retinoic acid in vivo and in vitro by tandem mass spectrometry. *Anal Chem*. 2008;80(5):1702–8. [PubMed: 18251521]

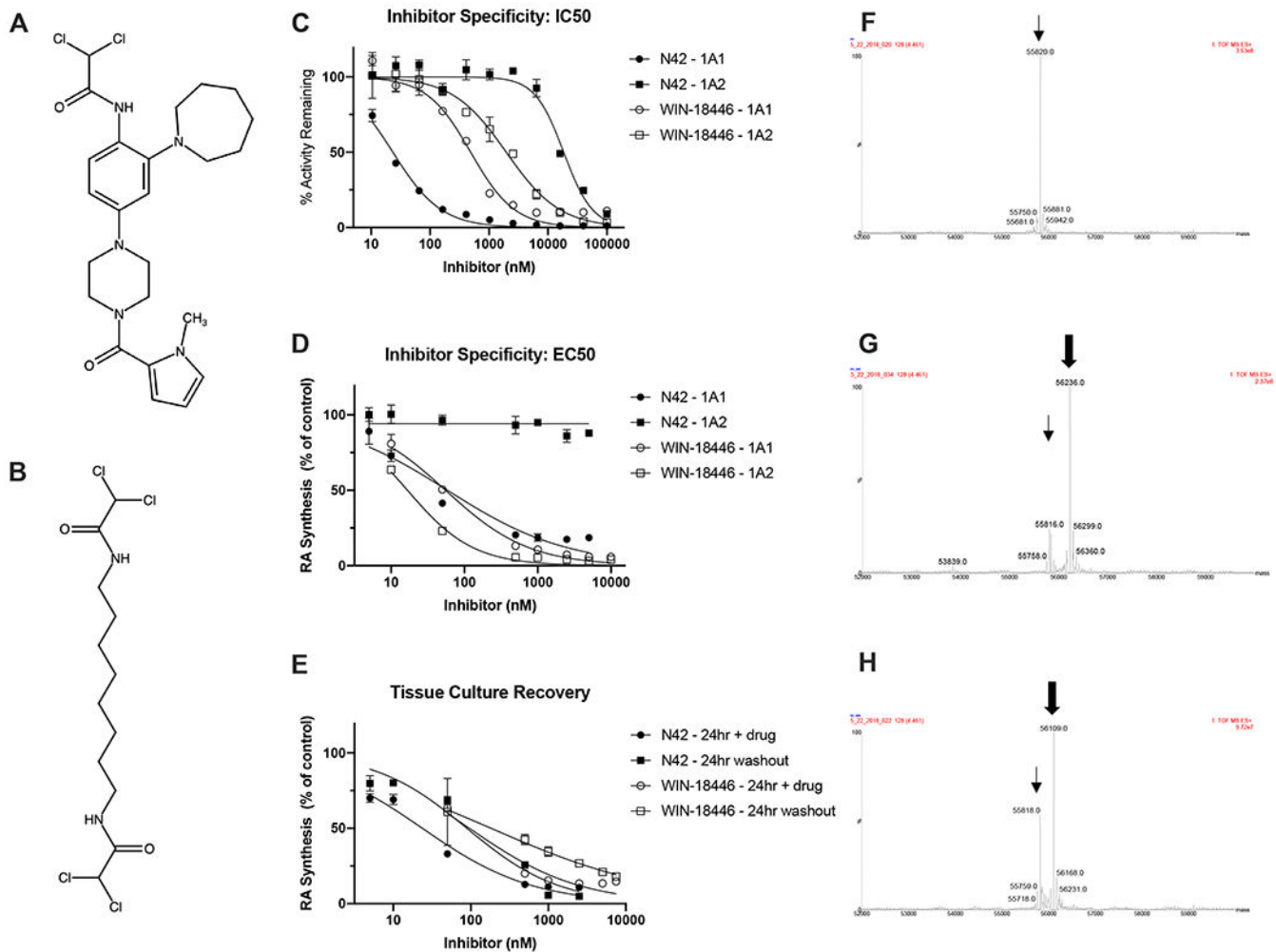


**Figure 1. Characterization of novel ALDH1A1 inhibitor, N42**  
 Structure of (A) ALDH1A1-specific inhibitor, N42 (mw, 492), and (B) pan-ALDH1A inhibitor, WIN18446 (mw, 366). (C) Potency and specificity of N42 compared to WIN18446 was examined (C) against recombinant ALDH1A1 and ALDH1A2 and (D) in H1299 cells expressing either ALDH1A1 or ALDH1A2. For recombinant enzymes, rate of RA production was calculated and is expressed as % of ALDH1A1 or ALDH1A2 enzyme without inhibitor. For cell culture experiments, RA concentration in media was determined and expressed as % of control (without inhibitors). (E) Long-term effects of N42 were assessed by determining RA production in media of H1299 cells expressing ALDH1A1. Cells were incubated with retinaldehyde and varying concentrations of N42 or WIN18446 for 24 h. Cells were then washed and provided fresh media containing only retinaldehyde for additional 24 h. RA concentrations in media were determined and are expressed as % of control, i.e. cells cultured without inhibitor throughout the experimental period. Each data point is mean of triplicates (mean  $\pm$  SD) Each experiment was repeated 2-3 times. Result from one representative experiment is shown. (F-H) Strong binding of N42 to ALDH1A1 was shown by MSTOF. High-resolution mass-spectra of (F) ALDH1A1 (G) N42 +

ALDH1A1 (G) and (H) WIN18446 + ALDH1A1. Thin arrow, ALDH1A1; thick arrow, shifted mass due to binding of inhibitor to ALDH1A1.

Author Manuscript

Author Manuscript

Author Manuscript

Author Manuscript

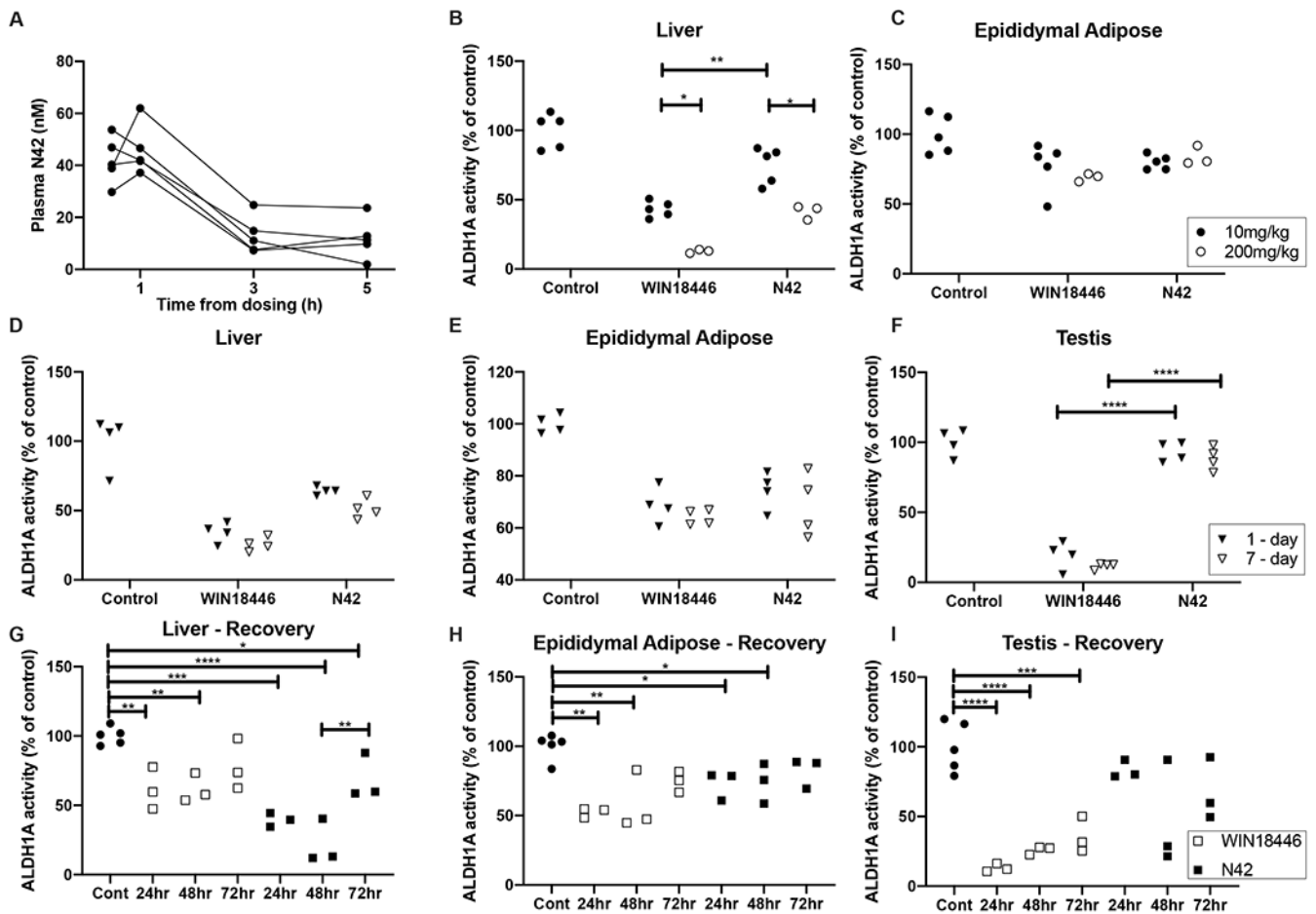


**Figure 2. Pharmacokinetics and pharmacodynamics of N42.**

(A) Plasma concentration of N42 was determined in mice after oral instillation at 10 mg/kg. (B, C) Short-term (5h) pharmacodynamics of N42 compared to WIN18446 were evaluated by assessing RA synthesis capacity of S10 fraction from (B) liver and (C) epididymal adipose of mice given 10 or 200 mg ALDH1A inhibitor/kg body weight. WIN18446 was used as a positive control. (D-F) Pharmacodynamics of N42 following single (1 day) and multiple dosing (7 days) were determined by assessing RA synthesis capacity from S10 fraction of (D) liver, (E) epididymal adipose and (F) testis 24 h after the last dosing. N42 or WIN18446 was given at 200 mg/kg body weight. (G-I) Long-term effects of N42 were determined by RA synthesis capacity of S10 fractions from (G) liver, (H) epididymal adipose and (I) testis in mice at 24, 48 and 72 h following a single oral dose of N42 or WIN18446 (200 mg/kg body weight). B-F, Two-way ANOVA followed by Tukey's or Sidak's post-hoc test for multiple comparisons. G-I, One-way ANOVA was performed followed by Tukey's post-hoc test for multiple comparisons, \*  $p < 0.05$ , \*\*  $p < 0.01$ , \*\*\*  $p < 0.001$ , \*\*\*\*  $p < 0.0001$ . Note that statistical significance was noted only between two different doses of the same drug or two different drugs, and significant differences between control and treatments are omitted in graphs B-F to avoid too many comparison bars. Detailed multiple comparison methods and results are provided in Supplement table 1.



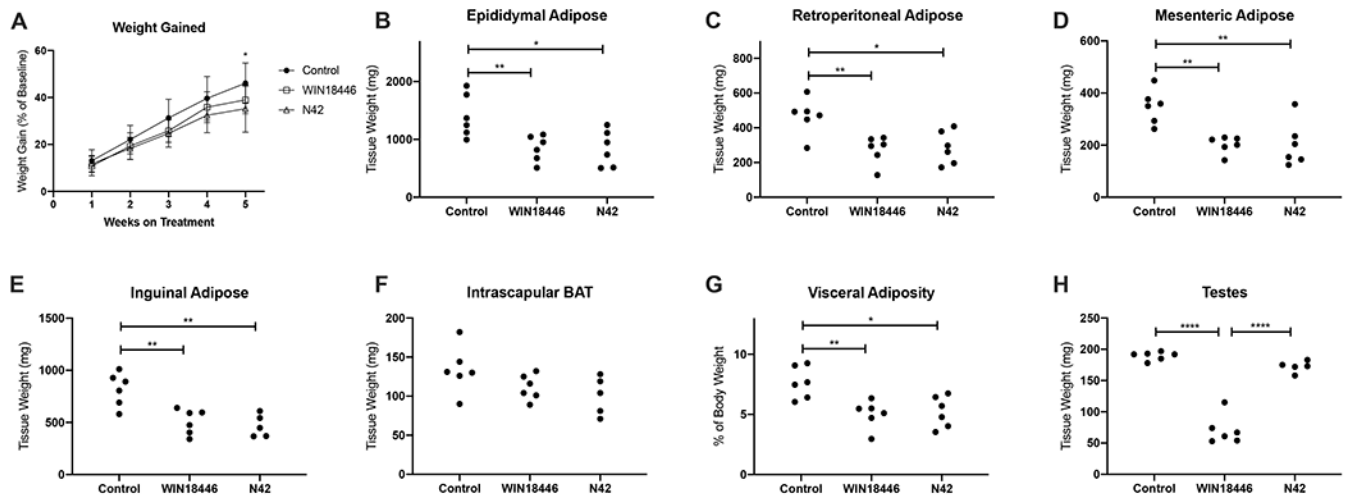


**Figure 3. Efficacy of N42 in reduction of weight gain in mice fed a HFD**

Mice were fed a HFD for 5 weeks and given daily oral doses of N42, WIN18446 or vehicle. (A) Body weight changes were assessed weekly. At the end of the study period, individual adipose depots were dissected and weighed: (B) epididymal adipose, (C) retroperitoneal adipose, (D) mesenteric adipose, (E) inguinal adipose, (F) intrascapular brown adipose tissue (BAT). (G) visceral adiposity was expressed as sum of three visceral adipose tissue weight / body weight X 100. (H) Testes weight was determined to assess effects of N42 compared to WIN18446. One-way ANOVA was performed followed by Tukey's post-hoc test for multiple comparisons, \*  $p < 0.05$ , \*\*  $p < 0.01$ , \*\*\*  $p < 0.001$ , \*\*\*\*  $p < 0.0001$

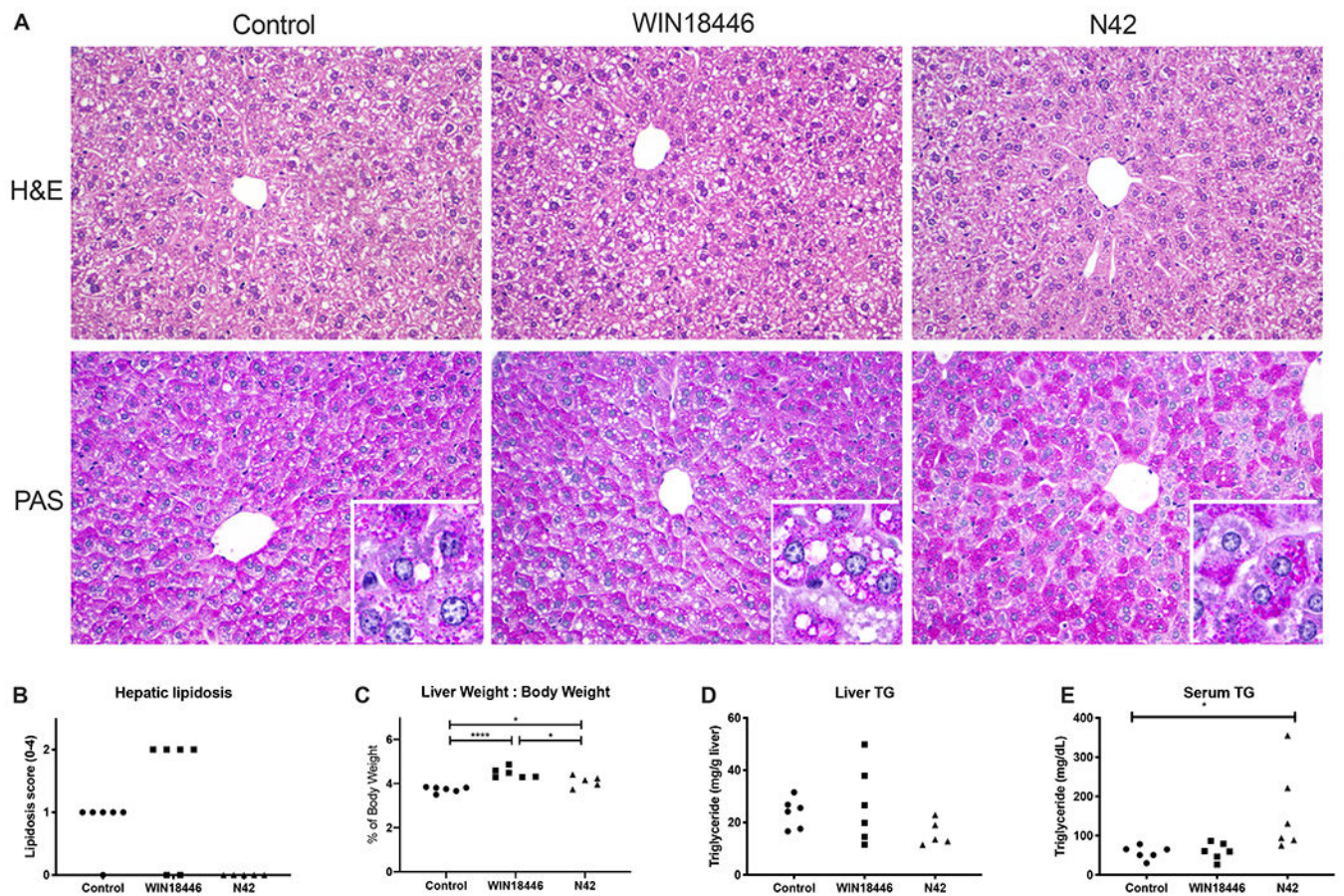


**Figure 4. Effects of N42 in hepatic lipidosis**

(A) Representative H&E (top row) and PAS stained liver sections. The hepatocytes of mice fed a HFD (control) have minimal macrovesicular lipidosis characterized by single large intracytoplasmic vacuoles within affected hepatocytes (median score, 1). In contrast, hepatocytes of mice fed a HFD and treated with WIN18446 have mild microvesicular lipidosis characterized by multiple small cytoplasmic vacuoles within affected hepatocytes (median score, 2). Hepatocytes of mice fed a HFD and treated with N42 contain no intracytoplasmic vacuoles (median score, 0). PAS-positive glycogen is displaced by vacuoles in the hepatocytes of control and WIN18446-treated mice but not in those of mice treated with N42. Insets original magnification 600X; all others 200X. (B) Hepatic lipidosis was scored by a veterinary pathologist blinded to treatment groups. (C) Ratio of liver weight : body weight was determined at 5 weeks following the treatment. Triglycerides of (D) liver and (E) serum were determined by colorimetric analysis. For hepatic lipidosis, non-parametric one-way ANOVA, Kruskal-Wallis, was performed followed by Dunn's post-hoc test for multiple comparisons. For all others, one-way ANOVA followed by Tukey's post-hoc test for multiple comparisons, \*  $p < 0.05$ , \*\*\*\*  $p < 0.0001$ .

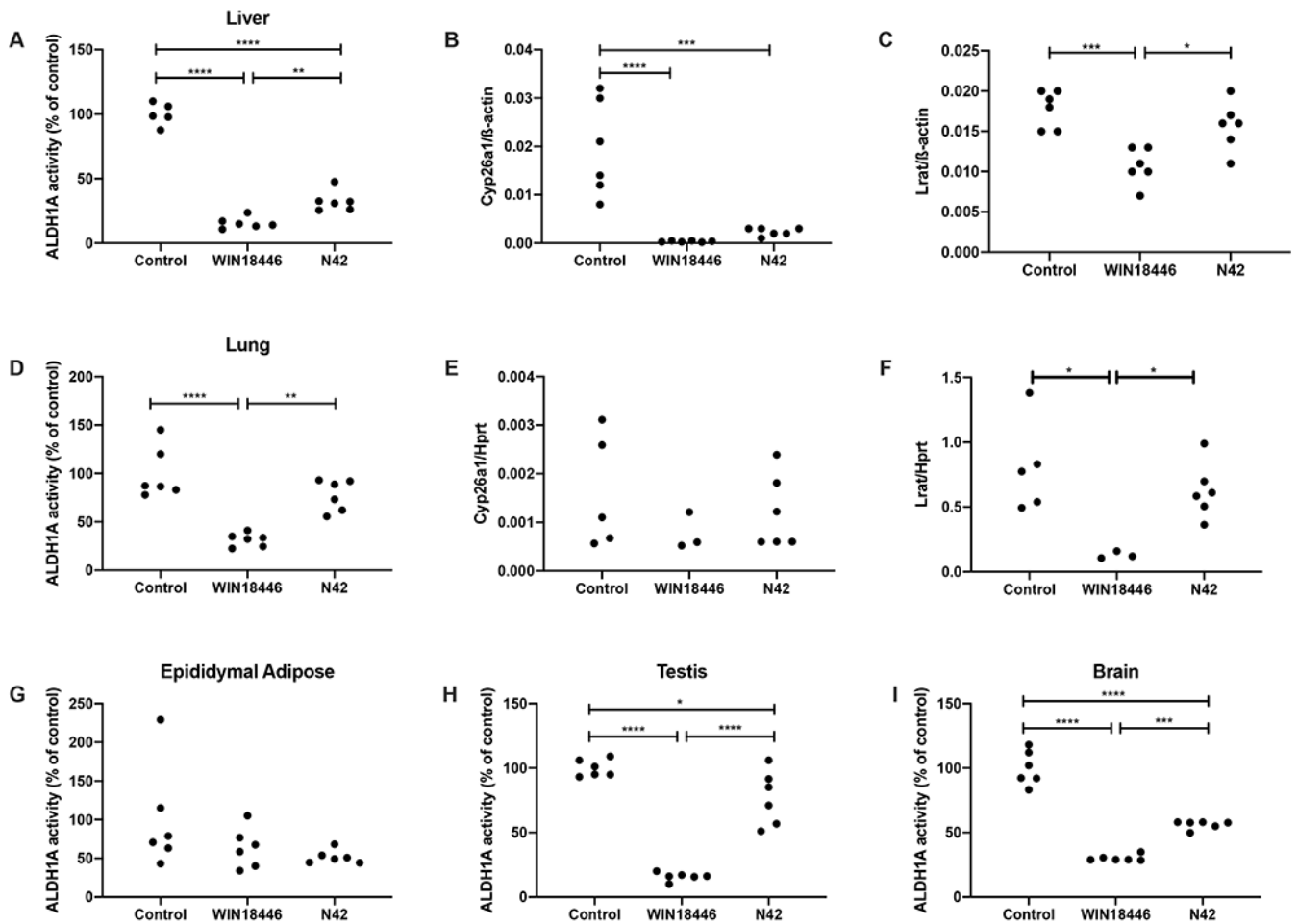


**Figure 5. Pharmacodynamic effects of N42 on RA synthesis in various tissues after 5 weeks of treatment**

Inhibitory effects of N42 on RA synthesis were assessed using S10 enzyme activity assay from (A) liver, (D) lung, (G) epididymal adipose, (H) testis, and (I) brain. Effects of RA reduction by N42 were analyzed by determining expression levels of RA-responsive genes, *Cyp26a1* in (B) liver and (E) lung; *Lrat* in (C) liver and (F) lung. One-way ANOVA was performed followed by Tukey's post-hoc test for multiple comparisons, \*  $p < 0.05$ , \*\*  $p < 0.01$ , \*\*\*  $p < 0.001$ , \*\*\*\*  $p < 0.0001$

**Table 1.**

Retinol and retinyl ester levels in liver and lung from mice after 5-week treatment (mean  $\pm$  SD). One-way ANOVA followed by Tukey's post-hoc test for multiple comparisons, compared to control.

Tissue	Retinoids	Treatment (n=6/group)		
		Control	WIN18446	N42
Liver	Retinyl esters (pmol/mg tissue)	870 $\pm$ 376	633 $\pm$ 79	735 $\pm$ 223
	Retinol (pmol/mg tissue)	29 $\pm$ 16	10 $\pm$ 5 *	17 $\pm$ 9
Lung	Retinyl esters (pmol/mg tissue)	95 $\pm$ 42	8 $\pm$ 3 ***	58 $\pm$ 17
	Retinol (pmol/mg tissue)	1.62 $\pm$ 0.76	0.41 $\pm$ 0.16 **	1.2 $\pm$ 0.34
Serum	Retinol ( $\mu$ M)	0.72 $\pm$ 0.05	0.71 $\pm$ 0.06	0.71 $\pm$ 0.06

\* , p<0.05;

\*\* , p<0.01;

\*\*\* , p<0.001